American Mineralogist, Volume 97, pages 1284–1290, 2012

Celadonite in continental flood basalts of the Columbia River Basalt Group

Leslie L. Baker,[1,2,*] William C. Rember,[2] Kenneth F. Sprenke,[2] and Daniel G. Strawn[1]

[1]Division of Soil and Land Resources, University of Idaho, Moscow, Idaho 83844-2339, U.S.A.
[2]Department of Geological Sciences, University of Idaho, Moscow, Idaho 83844-3022, U.S.A.

Abstract

Celadonite is a common alteration product of basalts in marine environments. It has been argued that marine fluids are necessary for celadonite formation, possibly by providing a source of K and other dissolved cations. Laterally extensive deposits of celadonite occur in basalts of the Grande Ronde Basalt of the Columbia River Basalt Group. The celadonite is found in scoriaceous flow tops of layered basalt flows, where it fills vesicles and replaces the surrounding groundmass. Evolved interstitial glasses are present in the basalts and dissolution of these glasses may provide sufficient K for celadonite formation, whereas dissolution of groundmass augite provides a source of Mg and Fe. These observations show that alteration by seawater or any other external source of dissolved ions is not necessarily required for celadonite formation.

Keywords: Celadonite, basalt alteration, Columbia River Basalts

Introduction

Celadonite is a dioctahedral phyllosilicate mineral of the mica group, with an ideal formula $K(Fe^{3+},Al)(Fe^{2+},Mg)Si_4O_{10}(OH)_2$. It has a distinctive blue-green color resulting from the presence of both Fe^{2+} and Fe^{3+} replacing Al in the octahedral sheet (Velde 2003). It shows limited Al substitution in the tetrahedral sheet, typically less than 0.2 atoms (Odin et al. 1988; Velde 2003), although aluminoceladonite and ferroaluminoceladonite are recognized mineral phases (Li et al. 1997; Rieder et al. 1999). Although both Fe^{2+} and Fe^{3+} are present, most (80–96%) Fe in celadonite is trivalent (Odin et al. 1988). Celadonite is most commonly formed by alteration of basaltic to intermediate rocks. It is frequently found as fracture or cavity-filling deposits in highly vesicular or porous basalts, or as a thin coating on altered basalt, and in more extensively altered basalts it may replace glass or phenocrysts. Celadonite in basalts typically occurs with other secondary alteration minerals including quartz, chalcedony, opal, calcite, nontronite, saponite, and zeolites such as clinoptilolite, heulandites, and laumontite (Andrews 1980; Alt and Honnorez 1984; Cummings et al. 1989; Neuhoff et al. 1999). Although glauconite often shows significant interstratification with smectites, interstratification of celadonite is considered uncommon (Odin et al. 1988; Velde 2003). Celadonite has also been shown to weather to Fe-rich smectite in soils by the loss of interlayer K (Reid et al. 1988).

It is generally held that most celadonite forms in a marine environment and that interaction with seawater provides a source of K (Odin et al. 1988; Weaver 1989; Velde 2003) and possibly of Mg (Andrews 1980). This is well enough accepted that celadonite occurring in non-marine rocks has been assumed to indicate a previous phase of marine alteration (Baker 1997). Celadonite is known to have formed in an entirely continental setting in a few cases, but these occurrences have not been as extensively documented as those of marine origin. Continental celadonite occurrences have been described in paleosols in the Eocene John Day Formation and the Miocene Picture Gorge Basalt of Oregon (Hay 1963; Retallack et al. 1999; Sheldon 2003), as well as at Olduvai Gorge (Hover and Ashley 2003), and in Australia (Norrish and Pickering 1983). Celadonite has also previously been described as a minor alteration product in Miocene basalts of the Columbia River group (Benson and Teague 1982; Cummings et al. 1989) and in an Oligocene basalt in south-central Washington (Wise and Eugster 1964). Celadonite is also described as a minor phase accompanying amethyst geodes in Brazilian basalts (Gilg et al. 2003), and deep groundwater was probably involved in its formation (Morteani et al. 2010), but a specific K source for this occurrence was not identified. Celadonite filling vesicles in Icelandic basalts has also been described (Neuhoff et al. 1999), with surface freshwater described as a potential source of K and Si.

Here we describe a locally extensive occurrence of celadonite that has formed by alteration of Miocene Grande Ronde Basalts of the Columbia River Basalt Group in Washington state, U.S.A. The petrology, chemistry, and stratigraphic relations of these tholeiitic basalts have been extensively studied (Ross 1978; Camp 1981; Reidel 1983; Mangan et al. 1986; Reidel et al. 1989; Caprarelli and Reidel 2004), but relatively few studies have examined their alteration mineralogy (Benson and Teague 1982; Trone 1986; Cummings et al. 1989; Hoover and Murphy 1989). These rocks were unquestionably erupted and weathered under nonmarine conditions (Hooper 1982). The objective of this study was to determine the source of K and other cations necessary for celadonite precipitation in the absence of seawater.

Samples and analytical methods

Samples were collected from the N1 magnetostratigraphic unit of the Grande Ronde member of the Columbia River Basalts, exposed in the Grande Ronde River canyon in Washington state, U.S.A. (Fig. 1). The canyon walls at the field site expose stacked basalt flows approximately 800 m in total thickness (Reidel 1983; Reidel et al. 1989), as well as feeder dikes for younger Grande Ronde Basalt flows. The N1 flows are between 16.5 and 15.6 million years old and are

* E-mail: lbaker@uidaho.edu

0003-004X/12/0809–1284$05.00/DOI: http://dx.doi.org/10.2138/am.2012.4129

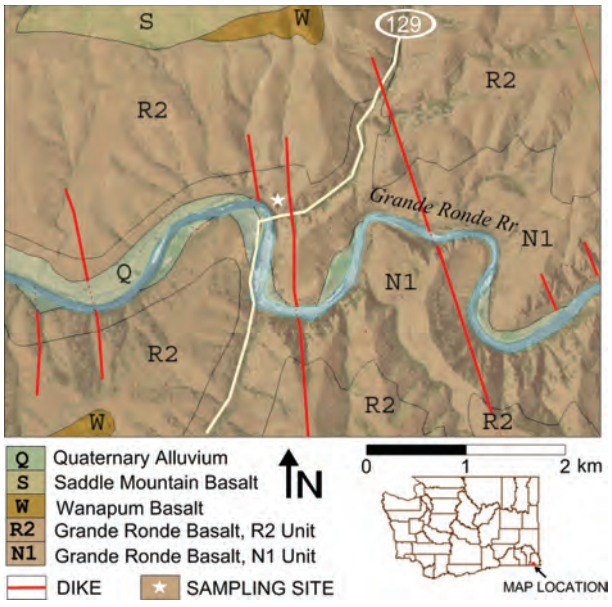

Figure 1. Geologic map of the sample location in the Grande Ronde River canyon in SE Washington, U.S.A., after Washington Division of Geology and Earth Resources (2005). The sample site (marked with star) is located within the N1 magnetostratigraphic unit of the Grande Ronde Basalt. (Color online.)

the lowermost basalts exposed at this location. Each successive flow has an easily identifiable scoriaceous top underlain by highly vesicular lavas that grade downward into blocky or columnar basalt. Small spiracles are occasionally present in flow bottoms. Vesicles, void spaces, and cracks in the scoriaceous flow tops are filled with secondary minerals including blue-green clays. One site, at the intersection of Washington Highway 129 and the Grande Ronde River Road (Fig. 1), was selected for further study. At this site, vesicle- and cavity-filling material was dominated by blue-green clays. Only the vesicle-filling blue-green clays from this site were examined in the present study.

Samples of altered basalt containing blue-green vesicle-filling material were collected for analysis. The analytical data presented here are of blue-green clay samples collected from individual vesicles. Samples were initially crushed by hand using a mortar and pestle and analyzed by diffuse reflectance Fourier transform infrared spectroscopy (FTIR), powder X-ray diffractometry (XRD), and scanning electron microscopy (SEM). For further analysis, selected samples were suspended in deionized water and the clay (<2 µm) size fraction was separated by centrifugation, washed in deionized water and freeze dried. The clay fraction was analyzed by SEM and was used to prepare oriented mounts for XRD clay mineralogy (Harris and White 2008). Thin sections of selected hand samples were prepared and examined optically and by SEM and electron microprobe.

Samples were prepared for FTIR by grinding a mixture of 3 wt% sample in optical grade KBr, and were analyzed using a Perkin Elmer diffuse reflectance accessory on a Perkin Elmer Spectrum 2000. A total of 100 spectra were collected, averaged, and processed using Perkin Elmer Spectrum 2.0 software. This software contains a built-in Kubelka-Munk algorithm for correcting diffuse reflectance spectra, and this algorithm was applied to all spectra. Infrared peak assignments were made following those in Besson and Drits (1997) and Drits et al. (1997). To determine cation composition of the octahedral sheet, infrared peaks in the OH-stretching range were fit using the peak deconvolution and fitting routines in Origin 8.5.1 (OriginLab Corporation, Northhampton, Massachusetts).

For bulk XRD, unpurified clays were crushed by hand using a mortar and pestle and packed into plastic sample holders. Samples were scanned on a Bruker D5000 diffractometer using Cu$K\alpha_1$ radiation at 40 kV and 30 mA, a step size of 0.050 °2θ, and a count time of 1.5 s per step. Scans were processed using the Bruker Diffracplus Eva evaluation software. For SEM analysis, clay fraction separates were mounted on doubly adhesive carbon tape and analyzed using a Zeiss Supra 35 field emission SEM. Thin sections of selected hand samples were analyzed on a JEOL field emission electron microprobe at Washington State University. Individual celadonite grains were analyzed using a 15 kV accelerating voltage, 30 nA beam current, and 3 µm spot size. Matrix glasses were analyzed using a 20 kV accelerating voltage, 15 nA beam current, and 7 µm spot size.

Results

The scoriaceous basalt hand samples contained phenocrysts of plagioclase, titanomagnetite, and augite. This mineralogy is typical of most Grande Ronde Basalts, including the N1 flows (Reidel et al. 1989). Numerous vesicles were coated or filled with blue-green clay (Fig. 2a). Some larger cavities were filled with other minerals including chalcedony, opal, and a zeolite. These mineralogical observations are consistent with those described by Trone (1986) at a different location in the Grande Ronde River valley. However, the samples described by Trone (1986) exhibited more textural complexity than the samples from this study. They observed scale-dependent variations in mineralogy as well as mineral zonation within filled void spaces. In this study, however, zonation was not observed in vesicle filling materials. Although many vesicles were completely filled with secondary minerals, considerable porosity remained in the rock and many fractures remained open, suggesting that permeability to groundwater was high throughout alteration.

In thin section, the basalt groundmass consisted of glass and microlites of plagioclase, augite, titanomagnetite, and apatite. Mesostasis glass was pale brown in thin section and appeared to be uniform except where locally altered to dark reddish-brown. Glass contents varied locally but were generally 10–20%. Well-defined brown glass droplets such as those described by Lambert et al. (1989) were not observed. Vesicles were filled with celadonite of botryoidal texture, and around some vesicles, veinlets of celadonite intruded into and replaced groundmass (Figs. 2b–2c,

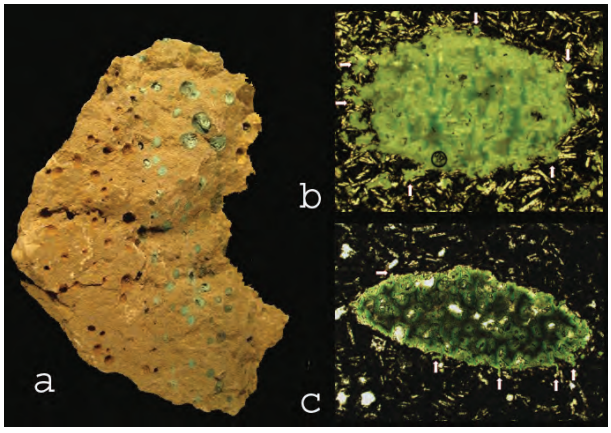

Figure 2. (**a**) Photograph of a hand sample of altered basalt showing vesicles coated or filled with blue-green celadonite. Sample is 10 cm across at its longest dimension. (**b**) Photomicrograph (plane-polarized light) of a green celadonite-filled vesicle in altered basalt sample GR1a, showing intrusion of celadonite into surrounding groundmass (arrows). The celadonite-filled void measures 1 mm across the long dimension. Phenocrysts and stringers of opaque titanomagnetite are visible within the green celadonite fill. (**c**) Photomicrograph (plane-polarized light) of a blue-green celadonite-filled vesicle in altered basalt sample GR1b, showing botryoidal texture of celadonite fill, and intrusion of celadonite into surrounding groundmass (arrows). The celadonite-filled void measures 1 mm across the long dimension. (Color online.)

arrows). This replacement sometimes affected regions much larger than the original vesicle, as indicated by rings of relict phenocrysts oriented around the previous locations of vesicle walls (Fig. 3). Plagioclase, titanomagnetite, and augite phenocrysts were embayed by celadonite replacing the surrounding groundmass but were not observed to have undergone replacement. No zonation was observed in thin sections or element maps of vesicle filling or groundmass-replacing material. Small (~1 μm) stringers of grains, opaque under the optical microscope and bright in backscatter and secondary electron images, were sometimes present in the vesicle filling material (Figs. 2b and 3). These grains had a high Fe content and were identified as Fe oxides, but they do not contain significant Ti, suggesting this was a separate oxide population from the accessory titanomagnetite present in the basalt. As such, they are likely to be a secondary phase formed during alteration.

Optical and SEM examination of grain mounts showed that the samples consisted of micrometer-sized needles similar to those illustrated in other studies (Odin et al. 1988). Individual needles were chemically analyzed by electron microprobe (Table 1). A structural formula was calculated from the average composition of Grande Ronde celadonite, renormalized to a water-free composition, using the constraint that the ferric-ferrous ratio in the octahedral sheet was adjusted to achieve charge balance. The resulting formula is $Si_{3.98}Al_{0.02}(Al_{0.15}Fe^{3+}_{1.02}Mg_{0.54}Fe^{2+}_{0.28})O_{10}(OH)_2(Ca_{0.02},K_{0.8})$, with a layer charge of 0.85 equivalents. This composition is consistent with an identification of the mineral as celadonite (Rieder et al. 1999). The Fe^{2+} content of the octahedral sheet, and the very low proportion of tetrahedral Al, are consistent with previously published analyses (Drits et al. 1997).

Electron microprobe analyses of mesostasis glass revealed that the elemental composition ranged from andesitic to rhyolitic (Table 1), with the most evolved compositions resembling the "clear glass" compositions published by Lambert et al. (1989) for interstitial glasses in Columbia River Basalts. Elemental concentrations in glasses within Grande Ronde Basalts have been shown to vary by several hundred percent over distances of a few centimeters due to quench fractionation (Hoover and Murphy 1989), so the variation among analyses shown in Table 1 is not unexpected.

Infrared spectra of several blue-green clays extracted from vesicle filling material are shown in Figure 4 and are consistent with published celadonite spectra (Velde 1978; Odin et al. 1988). Infrared band assignments in the OH-stretching region, following assignments made in Besson and Drits (1997) and Drits et al. (1997), are given in Table 2. An additional peak at 3681 cm^{-1}, present in some samples in which XRD scans indicated the presence of a smectite, was assigned to hydroxyl groups in saponite. This peak was not present in the smectite-free celadonite sample GR1a (Fig. 4). The peak fitting results from this sample are therefore shown in Table 2, because they are the least likely to be affected by non-celadonite peaks, although the fitting results did not differ greatly for other samples if baselines were carefully chosen. Because the Fe^{3+}-Mg-OH and the Al-Fe^{2+}-OH vibrations are given by Drits et al. (1997) and Besson and Drits (1997) as having identical vibration energies of 3559 cm^{-1}, the infrared peak at 3557 cm^{-1} (Fig. 4) was assigned 50% to each cation pair. This fitting suggests a composition for the octahedral sheet of $Al_{0.28}Fe^{3+}_{1.04}Mg_{0.50}Fe^{2+}_{0.19}$. The Fe^{3+} and Mg content of the octahedral sheet derived by this method are consistent with those calculated from the microprobe analyses; however, the Al and Fe^{2+} differ. This may be partly due to the assumptions made in

TABLE 1. Elemental compositions of celadonite and glass measured by electron microprobe

Celadonite	SiO_2	Al_2O_3	MgO	Fe_2O_3	CaO	Na_2O	K_2O	MnO	P_2O_5	TiO_2
GR1a8	55.46	1.76	5.02	23.99	0.24	n.d.	9.32	n.a.	n.a.	0.29
GR1a9	54.33	1.67	5.00	23.88	0.31	0.05	8.77	n.a.	n.a.	0.46
GR1a10	55.91	1.87	5.45	23.91	0.18	n.d.	9.55	n.a.	n.a.	0.07
GR1a11	53.88	2.40	4.73	21.85	0.27	n.d.	9.16	n.a.	n.a.	0.67
GR1e12	57.14	2.36	5.14	24.69	0.37	0.01	7.57	n.a.	n.a.	0.08
Average	55.34	2.01	5.07	23.66	0.27	0.01	8.88			0.31
(St.dev.)	(1.30)	(0.34)	(0.26)	(1.07)	(0.07)	(0.02)	(0.78)			(0.26)
Glass	SiO_2	Al_2O_3	MgO	FeO	CaO	Na_2O	K_2O	MnO	P_2O_5	TiO_2
GR1e1	74.62	13.08	0.02	1.60	0.37	3.46	6.52	0.02	0.12	1.01
GR1e2	77.29	11.73	0.10	1.54	0.88	3.26	4.95	0.01	0.28	0.49
GR1e3	76.11	12.09	0.05	2.40	0.24	3.24	6.24	0.00	0.07	0.83
GR1a1	65.77	15.01	0.20	4.94	2.87	4.90	3.43	0.06	0.70	1.45
GR1a2	63.89	14.97	0.30	6.42	2.98	4.99	3.05	0.08	0.60	1.33
GR1a4	68.12	14.46	0.26	5.16	2.84	4.60	3.36	0.07	0.64	0.93
6908 CGL*	74.4	14.1	0.3	1.8	2.1	1.8	6.1	0.0	0.0	0.8
6944 CGL*	75.4	13.4	0.4	1.1	0.3	3.5	5.8	0.0	0.0	0.2

Notes: n.a. = not analyzed; n.d. = not detected. Analyses from Lambert et al. (1989) of colorless matrix glasses of granitic composition in Grande Ronde Basalts are included for comparison.
* Colorless glass analyses reported by Lambert et al. (1989).

TABLE 2. Infrared peak assignments for sample GR1a (Fig. 2) after the method described by Besson and Drits (1997) and Drits et al. (1997), with the nominal peak locations given in those papers

Observed peak (cm^{-1})	Integrated absorbance	Assignment	Nominal peak (cm^{-1})
3602	2.10	Al-Mg-OH	3604
3579	1.89	Mg-Mg-OH	3583
3557	5.73	Fe^{3+}-Mg-OH or Al-Fe^{2+}-OH	3559
3533	6.06	Fe^{3+}-Fe^{3+}-OH	3535

Note: Integrated absorbances for each peak (in K-M units) were used to calculate the cation composition in the octahedral sheet.

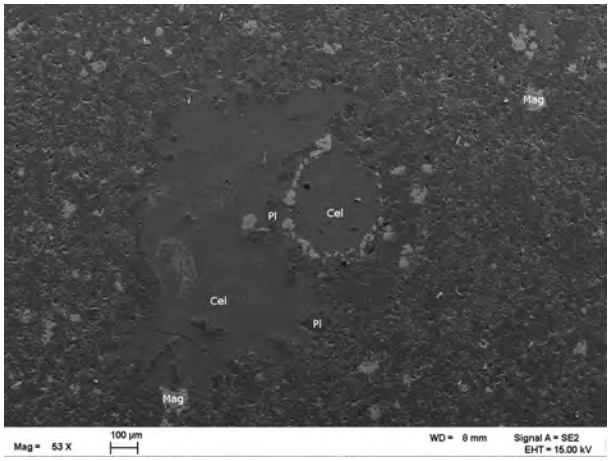

FIGURE 3. Secondary electron image of a vesicle in altered basalt sample GR1a, showing smooth-textured celadonite filling a vesicle (defined by the partial ring of titanomagnetite and plagioclase at center), replacing surrounding groundmass, and embaying remnant phenocrysts. Cel = celadonite, Pl = plagioclase, Mag = titanomagnetite. Thin stringers of bright material in the celadonite fill are Fe oxides with low-Ti content.

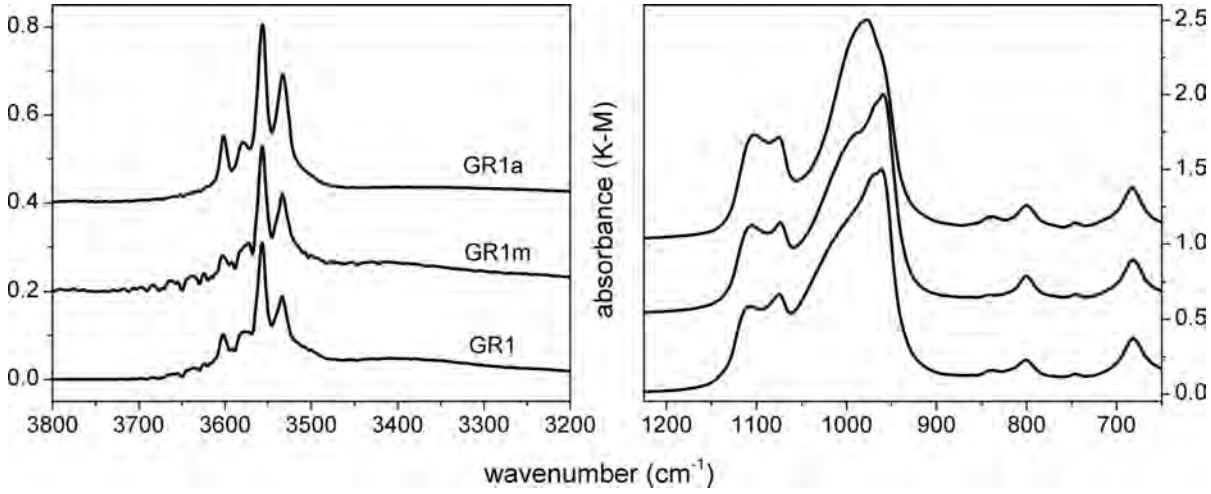

FIGURE 4. Infrared spectra of several vesicle-filling clays. Peak fitting results for sample GR1a are given in Table 2.

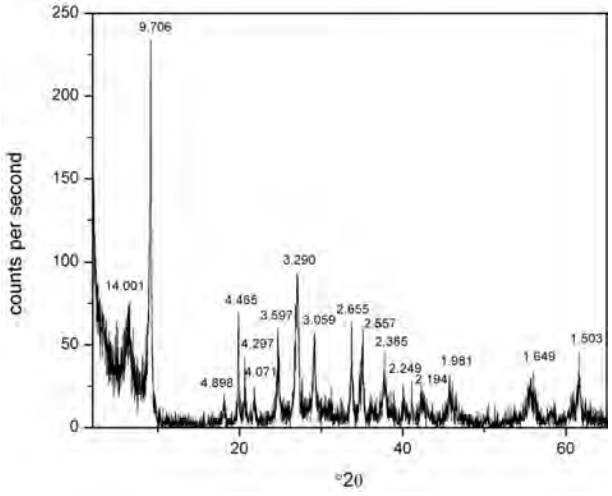

FIGURE 5. X-ray powder diffractogram of blue-green vesicle-filling clay sample GR1.

assigning the 3557 cm^{-1} peak and in calculating the formula from the microprobe analyses. It may also be due to small variations in celadonite composition among the different vesicle-filling materials (Table 1).

An XRD scan of a powder mount of a typical blue-green clay is shown in Figure 5, and is consistent with celadonite as the dominant mineral in the sample, based on published peak locations, intensities, and sharpness (Wise and Eugster 1964; Odin et al. 1988; Muller et al. 1999). XRD scans of other samples, not shown, display comparable celadonite peaks. The 060 peak, located at 1.503 Å in our samples (Fig. 5), is particularly useful for distinguishing celadonite from glauconite. For celadonite the 060 peak is reported as less than 1.510 Å, and in glauconite it is greater (Odom 1984). The diffractogram also indicates the presence of an additional smectite, probably saponite or nontronite, in some samples as shown by the presence of a peak at 14 Å that shifts with glycerol solvation and disappears with K saturation and heating (not shown). This smectite is likely responsible for the broad infrared peak centered near 3400 cm^{-1} (Fig. 4), which was not present in all samples analyzed. Some samples also contain minor clinoptilolite.

DISCUSSION

Celadonite formation in nonmarine basalts

As discussed above, it has frequently been asserted that celadonite formation during alteration of basalts requires an open system with seawater as a source of cations, particularly K. The Columbia River Basalts were erupted and weathered in a continental setting, so the cation supply for celadonite formation in these rocks must come entirely from dissolution of basaltic glass and minerals (in a closed system) or from circulating groundwater (in an open system). Because groundmass and mesostasis glass in the basalt samples were dissolved and replaced by celadonite, these materials represent a source of dissolved ions local to the alteration zone. Any deficit in cations necessary for celadonite formation must be satisfied by another source, such as circulating groundwater (Neuhoff et al. 1999; Gilg et al. 2003; Morteani et al. 2010). The Grande Ronde Basalts host an extensive aquifer, indicating significant permeability of these rocks on a regional scale. On a local scale, rubbly zones between flows, such as the altered rocks examined in this study, contain the majority of groundwater and are highly permeable, with joints controlling vertical groundwater communication between flow boundaries (Bortleson and Cox 1986), whereas the massive interiors of flows typically act as aquitards.

Mesostasis glasses of dacitic to rhyolitic composition such as those observed in the basalts under study have been previously described in other Grande Ronde Basalt flow units (Lambert et al. 1989), and their evolved compositions have been ascribed to quench fractionation (Hoover and Murphy 1989). These glasses contain elevated levels of K compared to the bulk composition of Grande Ronde Basalts, which ranges from 0.5 to 1.85 wt% K_2O (Reidel et al. 1989). The mesostasis glass that was dissolved and replaced around many vesicles is therefore one potential K source. Considerable variation exists in glass composition from

point to point (Table 1), but average glass contains 4.59 wt% K_2O and the most K-enriched point contains 6.52 wt% K_2O. The celadonite in these samples contains an average of 8.76 wt% K_2O. If dissolved glass was completely replaced by the same volume of pure celadonite, glass dissolution would provide approximately half the K necessary for celadonite formation, but this calculation does not account for celadonite precipitated in void spaces such as vesicles. Thus, additional K may be required, but not in excessively large amounts, particularly if glass is typically not replaced entirely by pure celadonite. If approximately half of the alteration assemblage consists of K-free phases such as opal, then there is apparently no significant K deficit. No attempt was made in this study to constrain the relative abundance of celadonite and K-free minerals in the bulk basalt, but qualitative observations suggest that the abundance of opal in the altered basalts is comparable to that of celadonite. Thus, the presence of an evolved, K-rich glass may enable celadonite formation in these basalts.

A potential external source of additional K and other dissolved cations for celadonite formation is silicic ash deposited during or between eruptions of the Grande Ronde Basalt flows. Anomalously high contents of K and other nutrient elements have been documented in paleosols in the Grande Ronde Formation and overlying Columbia River Basalts in central Washington, and have been ascribed to felsic ash input (Jolley et al. 2008). Similarly, paleosols in the Picture Gorge subgroup of the CRB show evidence of K metasomatism, the K source for which may have been felsic ash from regional explosive volcanism (Sheldon 2003). Neither of the cited studies directly observed ash particles in the sedimentary units they studied; rather, they inferred ash influence from geochemical observations. Regional explosive volcanism deposited silicic tephra in the Pacific Northwest throughout eruption of the Columbia River Basalts (Walker 1990; Hooper et al. 1995; Perkins et al. 1998) and volcanic ash is common in sedimentary interbeds between basalt flows, including within the Grande Ronde Basalts in central Washington and northern Oregon (Ross 1978; Smith 1988). Smith (2006) mapped a fused rhyolitic airfall tuff in a sedimentary interbed within the Grande Ronde N1 magnetostratigraphic unit. Although this tuff is not mapped as occurring at the sample collection locality, its mapped boundaries are geographically nearby, strongly suggesting some ash fell at the sample site. No tephra was directly observed between or in contact with the basalt flows sampled for this study, however. A complete mass-balance calculation, with analyses of unaltered as well as altered basalts, would be required to evaluate this hypothesis further.

In addition to K, Fe, and Mg are also necessary to form celadonite, but these elements are much less abundant than K in the mesostasis glass. Dissolution of the dacitic to rhyolitic mesostasis glass alone would provide only 10–25% of the necessary Fe and 1–4% of the necessary Mg to produce an equivalent amount of the observed celadonite composition (Table 1). Deposition of the secondary Fe oxides observed in some thin sections would require still more Fe. Augite crystals in the groundmass are a likely source of Fe and Mg. As discussed above, augite phenocrysts were sparse and were not observed to be altered or replaced by celadonite. Augite is present as microlites in the groundmass, however, and the nearly complete replacement of groundmass material surrounding some vesicles suggests that augite microlites underwent dissolution and replacement (Fig. 3). The dissolution of augite microlites but not of augite phenocrysts is likely due to the relatively high-surface area of the microlites. In quench-fractionated Grande Ronde Basalts, augite microlites in the groundmass contain a significant fraction of the bulk FeO content of the basalt (Hoover and Murphy 1989). As the only Mg-bearing mineral phase present, augite is also likely to contain the majority of the MgO in this sample. Thus, dissolution of augite microlites may account for the additional Fe and Mg necessary for celadonite precipitation in this system. However, some Fe and Mg may have been transported by groundwater from other sources. Present-day groundwater in the Grande Ronde aquifer contains up to 26 mg/L Mg and 94 µg/L Fe derived from interaction with the basalt (Bortleson and Cox 1986).

Conditions and timing of alteration

The lack of zonation observed in vesicle fill suggests that the altering fluid did not undergo major changes in composition. If groundmass dissolution was the primary source of dissolved ions for celadonite formation, then some dissolution must have preceded celadonite deposition. However, textural evidence suggests that some vesicle infill preceded extensive dissolution of groundmass. Rings of phenocrysts define the former locations of vesicle rims, now surrounded by celadonite (Fig. 3). Occasional phenocrysts occur in the center of the celadonite infill and are completely surrounded and embayed by it. If extensive dissolution had occurred before any celadonite precipitated, these mineral textures would not have been preserved. This textural evidence suggests a relatively slow and incremental process in which porewater chemistry was controlled by dissolution of groundmass and simultaneous precipitation of celadonite and accompanying minerals.

It has been observed that the oxidation state of groundwater reacting with Grande Ronde Basalts would be buffered by the FeO content of augite and titanomagnetite microlites in the groundmass during the early stages of alteration (Hoover and Murphy 1989). Odin et al. (1988) suggest that celadonite forms from altering fluids that circulate slowly, allowing the host basalt to buffer oxidation potential to slightly reducing conditions. This may be necessary to permit extensive substitution of Fe in the silicate structure rather than formation of a separate (oxyhydr)oxide phase (Velde 2003), unless ligands are present, which keep trivalent Fe in solution. However, most Fe in celadonites is Fe^{3+}, so oxidation must occur after Fe enters the silicate structure. Andrews (1980) used the position of the d_{003} peak of celadonite as an indicator of the oxygen fugacity under which it formed, applying the experimental results of Wise and Eugster (1964). The d_{003} spacing for celadonite in this study (Fig. 5) is 3.29, suggesting an oxygen fugacity slightly below the hematite-magnetite buffer. This estimate is consistent with the presence of unoxidized titanomagnetite embayed by celadonite in vesicles (Fig. 3). The two estimates of the octahedral sheet composition discussed above give ferric-ferrous ratios of 3.6 to 5.5 for celadonite in this study, also suggesting that it equilibrated at fairly oxidizing conditions.

The assemblage celadonite-silica-clinoptilolite-smectite suggests that alteration temperatures were low. This is in agree-

ment with the conclusions of Benson and Teague (1982), who in a study of alteration minerals in core samples of Grande Ronde Basalts, observed the same alteration assemblage forming textures similar to those in this study. They interpreted their data as indicating the alteration assemblage was produced by diagenesis under conditions similar to those that still prevail in the deep Grande Ronde aquifer, with temperatures of 15–35 °C and oxygen fugacity buffered by interaction with the basalt. The present-day composition of groundwater in the Grande Ronde Basalt aquifer is controlled by ongoing reaction with basalt and precipitation of calcite, clinoptilolite, opal, and Ca-Mg-rich clay minerals (Deutsch et al. 1982; Bortleson and Cox 1986). Thus, it may be that alteration of the Grande Ronde Basalts has proceeded slowly since the basalts were emplaced and continues to the present day.

An alternative set of formation conditions was proposed by Trone (1986) and Cummings et al. (1989). They suggest that alteration of these Grande Ronde Basalt flows occurred shortly after their emplacement. They and Orzol (1987) observed features that strongly suggest the altered basalt flow tops were water-saturated when the overlying flows were emplaced. They propose that the trapped porewater was the altering fluid, that alteration occurred due to heat input by the overriding basalt flow, and that alteration ceased upon cooling of the system. They also observed zoned textures and spatial variations in alteration mineralogy suggestive of a changing fluid composition over time. Thus, this presents an alternative model to that of Benson and Teague (1982). In this study, we did not observe variations in mineralogy or texture that suggested changing fluid composition; rather, it appeared that the composition of the altering fluid was buffered by basalt groundmass dissolution and precipitation of celadonite and possibly other phases. However, this may indicate simply that fluid circulation in our samples was more restricted than in the samples studied by Trone (1986), who observed variations in porosity even within individual breccia clasts.

Celadonite has been proposed as a possible phase contributing to remotely sensed spectra from phyllosilicate deposits on Mars (Bishop et al. 2008; McKeown et al. 2009). Although the formation conditions of the martian deposits are currently poorly constrained, they are unlikely to have occurred in a sub-seafloor environment (Noe Dobrea et al. 2010). The Grande Ronde celadonite occurrence may offer a better analog than seafloor basalts for possible celadonite on Mars.

Acknowledgments

This work was funded in part by a Research Initiation Grant from the Idaho Space Grant Consortium. We thank Michael Rowe for performing the electron microprobe analyses, Tom Williams for assistance with imaging, and Mickey Gunter and two referees for helpful comments on the manuscript.

References cited

Alt, J. and Honnorez, J. (1984) Alteration of the upper oceanic crust, DSDP site 417: mineralogy and chemistry. Contributions to Mineralogy and Petrology, 87, 149–169.

Andrews, A.J. (1980) Saponite and celadonite in Layer 2 basalts, DSDP Leg 37. Contributions to Mineralogy and Petrology, 73, 323–340.

Baker, J.C. (1997) Green ferric clay in non-marine sandstones of the Rewan Group, southern Bowen Basin, eastern Australia, Clay Minerals, 32, 4, 499–506.

Benson, L.V. and Teague, L.S. (1982) Diagenesis of basalts from the Pasco Basin, Washington; I, Distribution and composition of secondary mineral phases, Journal of Sedimentary Research, 52, 595–613.

Besson, G. and Drits, V.A. (1997) Refined relationships between chemical composition of dioctahedral fine-grained mica minerals and their infrared spectra within the OH stretching region; Part I, Identification of the OH stretching bands. Clays and Clay Minerals, 45, 158–169.

Bishop, J.L., Noe Dobrea, E.Z., McKeown, N.K., Parente, M., Ehlmann, B.L., Michalski, J.R., Milliken, R.E., Poulet, F., Swayze, G.A., Mustard, J.F., Murchie, S.L., and Bibring, J.-P. (2008) Phyllosilicate diversity and past aqueous activity revealed at Mawrth Vallis, Mars. Science, 321, 830–833.

Bortleson, G.C. and Cox, S.E. (1986) Occurrence of dissolved sodium ground waters in basalts underlying the Columbia Plateau, Washington. USGS Water-Resources Investigations Report 85-4005. U.S. Geological Survey, Tacoma, Washington.

Camp, V.E. (1981) Geologic studies of the Columbia Plateau: Part II. Upper Miocene basalt distribution, reflecting source locations, tectonism, and drainage history in the Clearwater embayment, Idaho. Geological Society of America Bulletin, 92, 669–678.

Caprarelli, G. and Reidel, S.P. (2004) Physical evolution of Grande Ronde Basalt magmas, Columbia River Basalt Group, north-western USA. Mineralogy and Petrology, 80, 1–25.

Cummings, M.L., Trone, P.M., and Pollock, J.M. (1989) Geochemistry of colloidal silica precipitates in altered Grande Ronde Basalt, northeastern Oregon, U.S.A. Chemical Geology, 75, 61–79.

Deutsch, W.J., Jenne, E.A., and Krupka, K.M. (1982) Solubility equilibria in basalt aquifers: The Columbia Plateau, eastern Washington, U.S.A. Chemical Geology, 36, 15–34.

Drits, V.A., Dainyak, L.G., Muller, F., Besson, G., and Manceau, A. (1997) Isomorphous cation distribution in celadonites, glauconites and Fe-illites determined by infrared, Moessbauer and EXAFS spectroscopies. Clay Minerals, 32, 153–179.

Gilg, H., Morteani, G., Kostitsyn, Y., Preinfalk, C., Gatter, I., and Strieder, A. (2003) Genesis of amethyst geodes in basaltic rocks of the Serra Geral Formation (Ametista do Sul, Rio Grande do Sul, Brazil): a fluid inclusion, REE, oxygen, carbon, and Sr isotope study on basalt, quartz, and calcite. Mineralium Deposita, 38, 1009–1025.

Harris, W. and White, G.N. (2008) X-ray diffraction techniques for soil mineral identification. In A.L Ulery and L.R. Drees, Eds., Methods of Soil Analysis, Part 5. Mineralogical Methods, p. 81–115. Soil Science Society of America, Madison, Wisconsin.

Hay, R.L. (1963) Stratigraphy and zeolitic diagenesis of the John Day formation of Oregon, University of California Press, Berkeley.

Hooper, P.R. (1982) The Columbia River Basalts, Science, 215, 4539, 1463–1468.

Hooper, P.R., Bailey, D.G., and Holder, G.A.M. (1995) Tertiary calc-alkaline magmatism associated with lithospheric extension in the Pacific Northwest. Journal of Geophysical Research, 100, 10303–10319.

Hoover, J.D. and Murphy, W.M. (1989) Quench fractionation in Columbia River basalt and implications for basalt-ground water interaction, In S.P. Reidel and P.R. Hooper, Eds., Volcanism and Tectonism in the Columbia River Flood-basalt Province, p. 307–320, Geological Society of America Special Paper 239, Boulder, Colorado.

Hover, V.C. and Ashley, G.M. (2003) Geochemical signatures of paleodepositional and diagenetic environments: A STEM/AEM study of authigenic clay minerals from an arid rift basin, Olduvai Gorge, Tanzania. Clays and Clay Minerals, 51, 231–251.

Jolley, D.W., Widdowson, M., and Self, S. (2008) Volcanogenic nutrient fluxes and plant ecosystems in large igneous provinces: an example from the Columbia River Basalt Group. Journal of the Geological Society, 165, 955–966.

Lambert, R.S.J., Marsh, I.K., and Chamberlain, V.E. (1989) The occurrence of interstitial granite-glass in all formations of the Columbia River Basalt Group and its petrogenetic implications. In S.P. Reidel and P.R. Hooper, Eds., Volcanism and Tectonism in the Columbia River Basalt Province, p. 321–332. Geological Society of America Special Paper 239. Geological Society of America, Denver, Colorado.

Li, G., Peacor, D.R., Coombs, D.S., and Kawachi, Y. (1997) Solid solution in the celadonite family; the new minerals ferroceladonite, $K_2Fe^{2+}_2Fe^{3+}_2Si_8O_{20}(OH)_4$, and ferroaluminoceladonite, $K_2Fe^{2+}_2Al_2Si_8O_{20}(OH)_4$. American Mineralogist, 82, 503–511.

Mangan, M.T., Wright, T.L., Swanson, D.A., and Byerly, G.R. (1986) Regional correlation of Grande Ronde Basalt flows, Columbia River Basalt Group, Washington, Oregon, and Idaho. Geological Society of America Bulletin 97, 1300–1318.

McKeown, N.K., Bishop, J.L., Noe Dobrea, E.Z., Ehlmann, B.L., Parente, M., Mustard, J.F., Murchie, S.L., Swayze, G.A., Bibring, J.-P., and Silver, E.A. (2009) Characterization of phyllosilicates observed in the central Mawrth Vallis region, Mars, their potential formational processes, and implications for past climate. Journal of Geophysical Research 114, E00D10.

Morteani, G., Kostitsyn, Y., Preinfalk, C., and Gilg, H. (2010) The genesis of the amethyst geodes at Artigas (Uruguay) and the paleohydrology of the Guaraní aquifer: structural, geochemical, oxygen, carbon, strontium isotope and fluid inclusion study. International Journal of Earth Sciences, 99, 927–947.

Muller, F., Plançon, A., Besson, G., and Drits, V.A. (1999) Nature, proportion and distribution of stacking faults in celadonite minerals. Materials Structure, 6, 129–134.

Neuhoff, P.S., Fridriksson, T., Arnorsson, S., and Bird, D.K. (1999) Porosity evolution and mineral paragenesis during low-grade metamorphism of basaltic lavas at Teigarhorn, eastern Iceland. American Journal of Science, 299, 467–501.

Noe Dobrea, E.Z., Bishop, J.L., McKeown, N.K., Fu, R., Rossi, C.M., Michalski, J.R., Heinlein, C., Hanus, V., Poulet, F., Mustard, R.J.F., and others. (2010) Mineralogy and stratigraphy of phyllosilicate-bearing and dark mantling units in the greater Mawrth Vallis/west Arabia Terra area: Constraints on geological origin, Journal of Geophysical Research, 115, E00D19.

Norrish, K. and Pickering, J.G. (1983) Clay Minerals. CSIRO: Melbourne/Academic Press, London.

Odin, G.S., Desprairies, A., Fullagar, P.D., Bellon, H., Decarreau, A., Frohlich, F., and Zelvelder, M. (1988) Nature and geological significance of celadonite. In G.S. Odin, Ed., Developments in Sedimentology, p. 337–398. Elsevier, Amsterdam.

Odom, I.E. (1984) Glauconite and celadonite minerals. In S.W. Bailey, Ed., Micas, vol. 13, p. 545–584. Reviews in Mineralogy and Geochemistry, Mineralogical Society of America, Chantilly, Virginia.

Orzol, L.L. (1987). Explosion structures in Grande Ronde Basalt of the Columbia River Basalt Group, near Troy, Oregon. M.S. thesis, Portland State University, Portland, Oregon, 220 p.

Perkins, M.E., Brown, F.H., Nash, W.P., Williams, S.K., and McIntosh, W. (1998) Sequence, age, and source of silicic fallout tuffs in middle to late Miocene basins of the northern Basin and Range province, Geological Society of America Bulletin, 110, 344–360.

Reid, D.A., Graham, R.C., Edinger, S.B., Bowen, L.H., and Ervin, J.O. (1988) Celadonite and its transformation to smectite in an Entisol at Red Rock Canyon, Kern County, California. Clays and Clay Minerals, 36, 5, 425–431.

Reidel, S.P. (1983) Stratigraphy and petrogenesis of the Grande Ronde Basalt from the deep canyon country of Washington, Oregon, and Idaho. Geological Society of America Bulletin 94, 4, 519–542.

Reidel, S.P., Tolan, T.L., Hooper, P.R., Beeson, M.H., Fecht, K.R., Bentley, R.D. and Anderson, J.L. (1989) The Grande Ronde Basalt, Columbia River Basalt Group—stratigraphic descriptions and correlations in Washington, Oregon, and Idaho. In S.P. Reidel and P.R. Hooper, Eds., Volcanism and Tectonism in the Columbia River Flood-basalt Province, p. 21–53. Geological Society of America Special Paper 239, Boulder, Colorado.

Retallack, G.J., Bestland, E.A., and Fremd, T.J. (1999) Eocene and Oligocene Paleosols of Central Oregon. Geological Society of America, Boulder, Colorado.

Rieder, M., Cavazzini, G., D'Yakonov, Y.S., Frank-Kamenetskii, V.A., Gottardi, G., Guggenheim, S., Koval, P.V., Mueller, G., Neiva, A.M.R., Radoslovich, E.W., Robert, J.L., Sassi, F.P., Takeda, H., Weiss, Z., and Wones, D.R. (1999) Nomenclature of the micas, Mineralogical Magazine, 63, 2, 267–279.

Ross, M.E. (1978) Stratigraphy, structure, and petrology of Columbia River basalt in a portion of the Grande Ronde River-Blue Mountains area of Oregon and Washington. Ph.D. dissertation, University of Idaho, Moscow, 407 p.

Sheldon, N.D. (2003) Pedogenesis and geochemical alteration of the Picture Gorge subgroup, Columbia River basalt, Oregon, Geological Society of America Bulletin 115, 11, 1377–1387.

Smith, G.A. (1988) Sedimentology of proximal to distal volcaniclastics dispersed across an active foldbelt: Ellensburg Formation (late Miocene), central Washington, Sedimentology, 35, 953–977.

Smith, S.V. (2005) Distribution, paleodrainage, and paleoclimate of the Miocene Columbia River Basalt Group and associated sedimentary interbeds in the Clearwater Embayment of west-central Idaho and southeastern Washington, 179 p. Ph.D. dissertation, Washington State University, Pullman.

Trone, P.M. (1986) Textural and mineralogical characteristics of altered Grande Ronde Basalt, northeastern Oregon: A natural analog for a nuclear waste repository in basalt. M.S. thesis, Portland State University, Portland, Oregon, 152 p.

Velde, B. (1978) Infrared spectra of synthetic micas in the series muscovite-MgAl celadonite. American Mineralogist, 63, 343–349.

——— (2003) Green clay minerals, In F.T. MacKenzie, Ed., Sediments, Diagenesis, and Sedimentary Rocks, p. 309–324. Pergamon, Oxford.

Walker, G.W. (1990) Miocene and younger rocks of the Blue Mountains region, exclusive of the Columbia River basalt group and associated mafic lava flows. In G.W. Walker, Ed., Geology of the Blue Mountains Region of Oregon, Idaho, and Washington: Cenozoic Geology of the Blue Mountains Region, p. 101–118. U.S. Geological Survery Professional Paper 1437, Denver, Colorado.

Washington Division of Geology and Earth Resources (2005) Digital 1:100,000-scale geology of Washington State, version 1.0. Open File Report 2005-3. Olympia, Washington.

Weaver, C.E. (1989) Clays, Muds, and Shales. Elsevier, Amsterdam.

Wise, W.S. and Eugster, H.P. (1964) Celadonite: Synthesis, thermal stability and occurrence. American Mineralogist, 49, 1031–1083.

Manuscript received February 9, 2012
Manuscript accepted May 18, 2012
Manuscript handled by Warren Huff